

Production and Correlations of Charged Particles with High P_t in 200-GeV/c $\pi^\pm p$, $K^- p$, and pp Collisions

C. Bromberg,^(a) G. Fox, R. Gomez, J. Pine, S. Stampke, and K. Yung
California Institute of Technology, Pasadena, California 91125

and

S. Erhan, E. Lorenz,^(b) M. Medinnis, J. Rohlf,^(c) and P. Schlein
University of California, Los Angeles, California 90024

and

V. Ashford,^(d) H. Haggerty, R. Juhala,^(e) E. Malamud, and S. Mori
Fermi National Accelerator Laboratory, Batavia, Illinois 60510

and

R. Abrams, R. Delzenero, H. Goldberg, S. Margulies, D. McLeod, J. Solomon, and R. Stanek
University of Illinois at Chicago Circle, Chicago, Illinois 60680

and

A. Dzierba and W. Kropac^(f)
Indiana University, Bloomington, Indiana 47401
(Received 19 April 1979)

Results are presented on the production of single charged particles with transverse momentum in the range of 0.8–4.5 GeV/c in $\pi^\pm p$, $K^- p$, and pp collisions at 200 GeV/c and on correlations between the trigger particle and particles with opposite azimuthal angle.

High-transverse-momentum (P_t) production of hadrons is thought to proceed through hard constituent scattering. Earlier results¹ on collective high- P_t phenomena (i.e., “jets”) were obtained by us using a large-aperture calorimeter-triggered multiparticle spectrometer at the Fermi National Accelerator Laboratory. In this Letter, we present production cross sections for single charged particles with $0.8 < P_t < 4.5$ GeV/c and at 90° in the c.m. system, produced in 200-GeV/c $\pi^- p$, $\pi^+ p$, and pp collisions. The ratios of the cross section for the reaction $pp \rightarrow h^\pm + X$ to that for $\pi^- p \rightarrow h^\pm + X$ and of that for $\pi^+ p \rightarrow h^\pm + X$ to that for $\pi^- p \rightarrow h^\pm + X$ are presented for different combinations of secondary hadron charges. Also, positive-to-negative charge ratios of Čerenkov-identified secondary particles, as well as correlations between the charge of associated “away-side” particles (those on the opposite side in azimuth from the trigger particle) and the trigger-particle species, are given.

Details of the spectrometer and of the single-particle trigger used for the data presented here are found in Ref. 1. We note here that, in order to understand the properties of the trigger bias, data were recorded for several different calorimeter bias settings, corresponding to P_t lower limits as low as 1.75 GeV/c and as high as 3.0 GeV/c.

In general, a particle with P_t below the trigger threshold can trigger the calorimeter in any of three ways: (a) The observed energy loss in the calorimeter is an upward fluctuation; (b) the magnetic deflection can increase a particle’s laboratory angle and hence its apparent P_t ; or (c) an additional particle deposits energy in the same calorimeter cell. (a) and (b) are adequately accounted for in a Monte Carlo acceptance calculation, while (c) can be corrected for by observing any accompanying charged particles in the spectrometer. Accompanying neutral particles are less frequent and can be estimated. Further details on these points will be reported elsewhere,² although we comment that in the ratios the effects of systematic errors arising from the trigger bias tend to cancel. Specifically, systematic errors contribute less than $\pm 10\%$ to the total error and are usually small compared to the statistical errors. The error bars on the ratios include the estimated systematic errors.

The 22-cell Čerenkov counter \check{C}_1 , described in Ref. 1, was used to identify secondary particles wherever possible. For 70% of the data, \check{C}_1 was filled with air (K threshold ≈ 21 GeV/c) and the remainder of the time filled with a 2:1 helium-air mixture (K threshold ≈ 32 GeV/c). At ~ 0.1 rad in the laboratory (90° in the c.m. system),

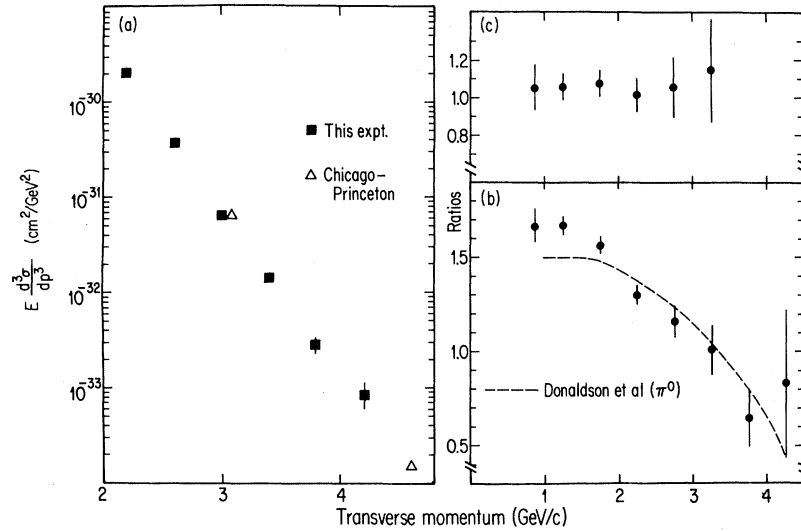


FIG. 1. (a) Inclusive invariant cross sections vs P_t for $pp \rightarrow \text{charged particle} + X$. Chicago-Princeton points are from Ref. 3. (b) Ratio of cross section in (a) to that for $\pi^- p \rightarrow \text{charged particle} + X$. Dashed curve is from Ref. 4. (c) Ratio of $\pi^+ p$ to $\pi^- p$ single-charged-particle cross sections.

π 's could be separated from a mixed K - p sample with P_t up to 3.2 GeV/c ; p 's (and also \bar{p} 's) could be separated from a mixed π - K sample with P_t greater than 2.1 GeV/c . Since particles with $\beta = 1$ produced an average of eight photoelectrons in air, pulse-height information could be used to identify π 's with $P_t > 2.1 \text{ GeV}/c$ in these data; with helium-air corrections of up to 10–15% were necessary for π background in the K - p sample.

Figure 1(a) shows our measurement of the inclusive charged-particle cross section for pp collisions. The results agree with the corresponding data from Antreasyan *et al.*³ Figure 1(b) shows our ratio of the pp cross section to the corresponding $\pi^- p$ charged-particle cross section. This ratio is almost identical to the $(pp \rightarrow \pi^0)/(\pi^- p \rightarrow \pi^0)$ ratio of Donaldson *et al.*⁴ Moreover, our ratio of $\pi^+ p/\pi^- p$, which is seen in Fig. 1(c) to be P_t independent at a value near unity, also agrees with the Donaldson *et al.* results for π^0 production. The falloff of our $pp/\pi^- p$ ratio in Fig. 1(b) shows that there is a crossover of pp and pp single-particle cross sections near $P_t \approx 3 \text{ GeV}/c$.

The ratios of the single-particle cross-section components of pp interactions to $\pi^- p$ interactions are shown in Fig. 2(a) for like-sign trigger particles and in Fig. 2(b) for unlike-sign trigger particles; the same ratios for $\pi^+ p$ and $\pi^- p$ interactions are shown in Figs. 2(c) and 2(d). The curves show fits to the data of the function $(1 - x_\perp)^n$, where $x_\perp = P_t/P_t^{\text{max}}$. The presence of baryons in

the final state may complicate the interpretation of these results. However, since, as discussed below, the final-state baryon components in $\pi^- p$

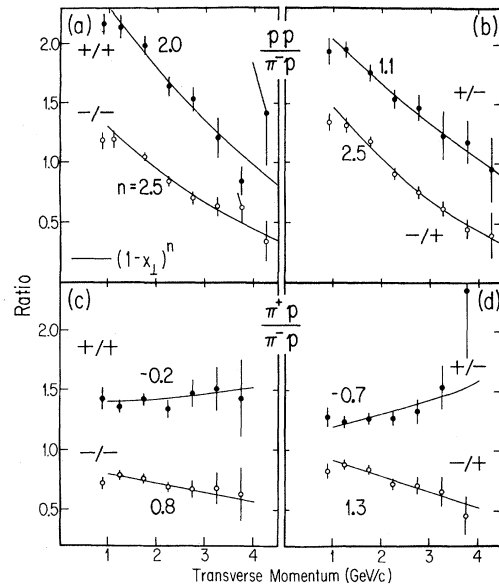


FIG. 2. Ratios of single-particle cross sections for indicated initial state and trigger-particle charge. Solid curves are fits of $(1 - x_\perp)^n$ to the data with $p_\perp > 1 \text{ GeV}/c$; the exponents, n , are shown; they have an uncertainty of ± 0.3 in (a) and (b), and ± 0.4 in (c) and (d). (a) $(pp \rightarrow h^+ + X)/(\pi^- p \rightarrow h^+ + X)$ and $(pp \rightarrow h^- + X)/(\pi^- p \rightarrow h^- + X)$; (b) $(pp \rightarrow h^+ + X)/(\pi^- p \rightarrow h^- + X)$ and $(pp \rightarrow h^- + X)/(\pi^- p \rightarrow h^+ + X)$; (c), (d) same as (a), (b) except for $\pi^+ p$ and $\pi^- p$ initial states.

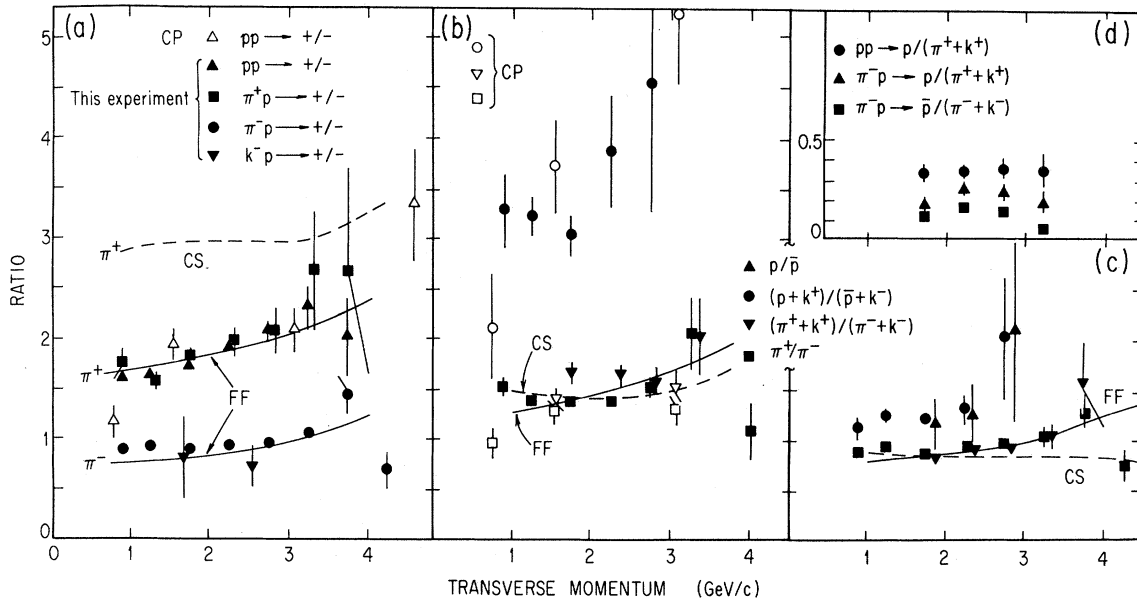


FIG. 3. (a) Trigger-particle charge-production ratio vs trigger-particle P_t for pp , π^+p , and K^-p reactions. Open symbols are from Ref. 3. FF and CS curves are from Refs. 5 and 8. (b) Charge ratios of indicated identified trigger particles for pp reactions. FF and CS curves are for $(pp \rightarrow \pi^+ + X)/(pp \rightarrow \pi^- + X)$. (c) Same as (b) except for π^-p reactions. (d) Proton/meson production ratios for indicated reactions.

and π^+p interactions are consistent with being nearly identical, the ratios displayed in Figs. 2(c) and 2(d) are essentially the ratios for π^+K production only. These latter ratios are seen to vary very slowly if at all with P_t .

Figure 3(a) shows the $+/-$ trigger charge ratio for pp , π^+p , and K^-p interactions versus P_t . The pp results agree well with those of CP.³ Despite differences in the initial-state quark content, π^+p is seen to have the same behavior as pp , and K^-p is similar to π^-p . Both the π^+p and π^-p results are seen to be correctly predicted by the early quantum chromodynamics (QCD) approximation of Field and Feynman⁵ (FF), although a quark-fusion⁶ constituent-interchange⁷ model (CIM) parametrization by Chase and Stirling⁸ (CS) is seen to disagree completely with the π^+p result. The CIM term alone in CS fits neither π^+p nor π^-p .

The results for the identified trigger particles are shown in Figs. 3(b)–3(d). The proton-beam data are seen to agree with the analogous results from CP³ and with the FF and CS predictions for $pp \rightarrow \pi + X$. We note that the ratio $(p+K^+)/(\bar{p}+K^-)$ is much larger than the π^+/π^- ratio for the proton-beam data, whereas for the π^- beam, the two ratios are comparable. This is presumably because protons contain none of the valence quarks necessary to form \bar{p} or K^- in the denominator of the first ratio. The p/\bar{p} ratio for the π^- beam is

seen to be close to unity, as compared with the larger p/\bar{p} ratio of 6 or more for the proton beam.³ This presumably also results from the valence-quark content of the initial state. Finally, Fig. 3(d) shows the proton/meson production ratios for the three reactions. None of the ratios appears to depend appreciably on P_t . The ratio for the lower-statistics π^+p data (not shown) agrees with the π^-p data.

We turn now to the charge correlations between "away-side" hadrons and the type of trigger particle.⁹ We define $R_a(h)$ as the away-side positive-to-negative charge-production ratio for all charged particles with c.m. production angle $45^\circ < \theta < 90^\circ$ and lying in a $\pm 45^\circ$ azimuthal wedge opposite the trigger particle; a is the incident beam particle and h is the trigger particle. In Fig. 4 we plot $R_a(\pi)$ and $R_a(K+p)$ for two different regions of $x_e = -\hat{p}_\perp^{\text{away}} \cdot \hat{p}_\perp^{\text{trig}} / p_\perp^{\text{trig}}$. We note that there is a dependence on x_e and, furthermore, that R_a appears to depend only on the charge of the trigger particle and not on its type, in agreement with QCD predictions.¹⁰

In a simple quark fragmentation model, a negative trigger in a π^-p collision increases the likelihood that the away quark came from a proton, while a positive trigger suggests that the away quark came from the π^- . Thus, we expect $R_{\pi^-}(h^+) < R_{\pi^-}(h^-)$, as observed. Further, since a

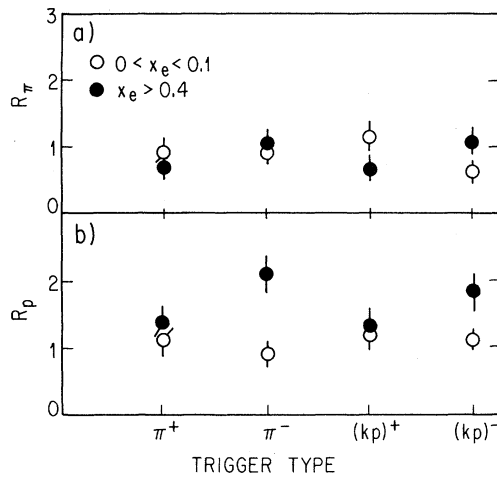


FIG. 4. The away-side charge production ratio for all away-side charged particles in the $\theta - \varphi$ acceptance region described in the text, for the indicated trigger-particle types: (a) for π^- -beam, (b) for proton-beam particle.

minus trigger can come either from the d quark in the incident proton or the d or \bar{u} quarks in the π^- , the denominator in $R_\pi(h^-)$ will be enhanced somewhat and we expect $R_\pi(h^-) < R_\pi(h^+)$, which is also seen. Thus the general pattern of the $x_e > 0.4$ data in Fig. 4 agrees with the qualitative predictions of the simple parton model, although the differences between $R_p(h^-)$ and $R_p(h^+)$ are larger than expected. A possible explanation is that all the residual valence quarks (those that do not directly participate in the hard scatter) influence the charge correlations on the far side. In other words, we are probably seeing contamination from the forward jet.¹¹ Whereas $x_e > 0.4$ should be large enough to eliminate contamination from the large- x_\parallel component of the forward jet, it is not large enough to eliminate the low- x_\parallel component. A detailed understanding of the quantitative features of the correlation data will have to await experiments at higher P_t , so that the contamination from the forward jet can be reduced.

We are grateful for the assistance given us by the staffs of the Accelerator Division, the Meson Department, and the Research Services Department at Fermilab. We thank B. Combridge, R. Field, and A. Pagnamenta for useful discussions. This work was supported in part by the U. S. National Science Foundation, the U. S. De-

partment of Energy, and the University of Illinois Research Board.

^(a)Present address: Michigan State University, East Lansing, Mich. 48824.

^(b)Visitor from the Max-Planck-Institut für Physik und Astrophysik, Munich.

^(c)Present address: California Institute of Technology, Pasadena, Cal. 91103.

^(d)Present address: Brookhaven National Laboratory, Upton, N. Y. 11973.

^(e)Present address: McDonnell-Douglas Corporation, St. Louis, Mo. 63121.

^(f)Present address: Hughes Aircraft Corporation, Los Angeles, Cal. 90024.

¹C. Bromberg *et al.*, Phys. Rev. Lett. **38**, 1447 (1977); and Nucl. Phys. **B134**, 189 (1978), and in *Proceedings of the Eighth International Symposium on Multiparticle Dynamics, Kaysersberg, France, 1977*, edited by R. Arnold, J. B. Gerber, and P. Schübelin (Centre National de la Recherche Scientifique, Strasbourg, France, 1977), p. B89, and Phys. Rev. Lett. **42**, 1202 (1979).

²See also M. Medinnis Ph.D. thesis University of California at Los Angeles (unpublished); R. Stanek Ph.D. thesis, University of Illinois, Chicago Circle (unpublished).

³D. Antreasyan *et al.*, Phys. Rev. Lett. **38**, 112, 115 (1977), and Phys. Rev. D **19**, 764 (1979), denoted by CP.

⁴G. Donaldson *et al.*, Phys. Rev. Lett. **36**, 1110 (1976).

⁵R. D. Field and R. P. Feynman, Phys. Rev. D **15**, 2590 (1977).

⁶P. V. Landshoff and J. C. Polkinghorne, Phys. Rev. D **10**, 891 (1974).

⁷R. Blankenbecler, S. J. Brodsky, and J. Gunion, Phys. Rev. D **12**, 3469 (1975).

⁸M. K. Chase and W. J. Stirling, Nucl. Phys. **B133**, 157 (1978).

⁹Similar data from pp collisions in different kinematic regions are available from CERN [K. H. Hansen, in *Proceedings of the Nineteenth International Conference on High Energy Physics, Tokyo, Japan, August 1978*, edited by S. Homma, M. Kawaguchi, and H. Miyazawa (Physical Society of Japan, Tokyo, 1979), p. 177] and Fermilab [R. J. Fisk *et al.*, Phys. Rev. Lett. **40**, 984 (1978)].

¹⁰R. P. Feynman, R. D. Field, and G. C. Fox, Phys. Rev. D **18**, 3320 (1978).

¹¹Theoretical descriptions of our correlation data should take into account our θ selection on the away side; the contribution of away-side quarks may be enhanced with respect to that of gluons because particles are selected in the forward hemisphere; this may help explain the large value of $R_p(h^-)$. See M. K. Chase, Phys. Lett. **79B**, 114 (1978).